of metal to the depth of down to 1 mm with formation of a characteristic groove of down to 0.14 mm depth. The size of the zone under the groove with considerable changes of grain shape (grain form factor $K_{f_{av}} = 11.8$) is equal to 200 μm.

3. At HFMP treatment of metal surface the load is applied by blocks of pulses of different width with maximum value of impact force in the block higher than 1000 N. Duration of such pulses of force impact does not exceed 100 μs, and frequency of their appearance is equal to approximately 1 kHz.

1. Zhao, X., Wang, D., Huo, L. (2011) Analysis of the S–N curves of welded joints enhanced by ultrasonic peening treatment. *Materials & Design*, 32(**1**), 88–96.
2. Abston, S. (2010) The technology and applications of ultrasonic impact technology. *Austral. Welding J.*, **55**, 20–21.
3. Yin, D., Wang, D., Jing, H. et al. (2010) The effects of ultrasonic peening treatment on the ultra-long life fatigue behavior of welded joints. *Materials & Design*, 31(**7**), 3299–3307.
4. Marquis, G. (2010) Failure modes and fatigue strength of improved HSS welds. *Eng. Fract. Mech.*, **77**, 2051–2062.
5. Wang, T., Wang, D., Huo, L. et al. (2009) Discussion on fatigue design of welded joints enhanced by ultrasonic peening treatment (UPT). *Int. J. Fatigue*, 31(**4**), 644–650.
6. Kudryavtsev, Y., Kleiman, J., Lugovskoy, A. et al. (2007) Rehabilitation and repair of welded elements and structures by ultrasonic peening. *Welding in the World*, 51(**7/8**), 47–53.
7. Kuhlmann, U., Duerr, A., Guenther, P. et al. (2005) Verlangerung der Lebensdauer von Schweisskonstruktion aus hoeherfesten Baustaehlen durch Anwendung der UIT-Technologie. *Schweissen und Schneiden*, 57(**8**), 384–391.
8. Huo, L., Wang, D., Zhang, Y. (2005) Investigation of the fatigue behaviour of the welded joints treated by TIG dressing and ultrasonic peening under variable-amplitude load. *Int. J. Fatigue*, 27(**1**), 95–101.
9. Statnikov, E.S., Muktepavel, V.O., Blomqvist, A. (2002) Comparison of ultrasonic impact treatment (UIT) and other fatigue life improvement methods. *Welding in the World*, 46(**3/4**), 20–32.
10. Mordvintseva, A.V. (1959) Ultrasonic impact treatment of welded joints for removal of residual stresses. *Trudy MVTU im. N.E. Baumana*, Issue 45, 32–43.
11. Lobanov, L.M., Kirian, V.I., Knysh, V.V. (2006) Improvement of fatigue resistance of welded joints in metal structures by high-frequency mechanical peening (Review). *The Paton Welding J.*, **9**, 2–8.
12. Prokopenko, G.I., Nedoseka, A.Ya., Gruzd, A.A. et al. (1995) Development and optimization of equipment and process of ultrasonic peening of welded joints for relaxation of residual stresses. *Tekhnich. Diagnostika i Nerazrush. Kontrol*, **3**, 14–22.
13. Kravtsov, T.G., Sevryukov, V.V. (2001) *Ultrasonic peening of ship parts and welded structures*. Nikolaev: UGMTU.
14. Nekhoroshov, O.N., Pershin, V.P., Semukhin, B.S. (2006) Application of ultrasonic peening method on welded joints of structural steels. *Vestnik TGA-SU*, **2**, 120–125.
15. Degtyaryov, V.A., Shulginov, B.S., Knysh, V.V. (2009) Deformation criterion of the efficiency of strengthening of welded joints by high-frequency mechanical peening. *The Paton Welding J.*, **10**, 39–41.
16. Mordyuk, B.N., Milman, Yu.V., Iefimov, M.O. et al. (2008) Characterization of ultrasonically peened and laser-shock peened surface layers of AISI-321 stainless steel. *Surface and Coating Technology*, **202**, 4875–4883.
17. Volosevich, P.Yu., Prokopenko, G.I., Knysh, V.V. et al. (2008) Structural changes in weld zone of St3 steel in ultrasonic peening and their influence on improvement of fatigue resistance. *Metallofizika i Nov. Tekhnologii*, 30(**10**), 1429–1443.
18. Mordyuk, B.N., Prokopenko, G.I. (2007) Ultrasonic impact peening for surface properties' management. *J. Sound and Vibrations*, 308(**3/5**), 855–866.
19. Volosevich, P.Yu., Kozlov, A.V., Mordyuk, B.N. et al. (2003) Plastic deformation in ultrasonic field and its possibilities as applied to carbon saturation of surface layers of iron specimens. *Metallofizika i Nov. Tekhnologii*, 25(**5**), 679–692.
20. Yurkova, A.I., Belotsky, A.V., Byakova, A.V. et al. (2007) Mechanism of iron dispersion in intensive plastic deformation by friction with simultaneous nitrogen diffusion. *Nanosistemy, Nanomaterialy, Nanotekhnologii*, 5(**2**), 565–588.
21. Mordyuk, B.N., Prokopenko, G.I. (2006) Fatigue life improvement of α-titanium by novel ultrasonically assisted technique. *Materials Sci. and Eng.*, **437**, 396–405.

SIMULATION OF THE EFFECT OF HIGH-VOLTAGE CABLES ON CURRENT RIPPLE IN WELDING GUNS WITH AUTOMATIC BIAS

O.K. NAZARENKO, V.A. MATVEJCHUK and **V.V. GALUSHKA**
E.O. Paton Electric Welding Institute, NASU, Kiev, Ukraine

The mechanism of formation of current ripple in welding electron guns with automatic bias caused by ripple of the cathode bombardment current is studied by using computer mathematical simulation. It is shown that when using the coaxial high-voltage cable the ripple of the cathode bombardment current does not affect the ripple of the beam current. In case of a multi-core cable or four separate single-core high-voltage cables the ripple of the cathode bombardment current causes the ripple of the beam current because of the parasitic capacitance currents flowing through the beam current control circuit. To decrease the beam current ripple factor to 0.05, the cathode bombardment current ripple factor at a frequency of 20 kHz should not exceed 0.05 either.

Keywords: *electron beam welding, high-voltage cable, distributed capacitances, electron gun, triode emission system, automatic bias, cathode bombardment current ripple, beam current ripple*

Despite the high-usage pulse modulation of the electron beam current with a depth of 100 %, it is important that in the steady-state operation mode the peak-to-peak amplitude of the beam current ripple be no more than 5 % (ripple factor 0.05), which is specified by international standard EN ISO 14744-1 [1]. This requirement is caused, in particular, by the need to

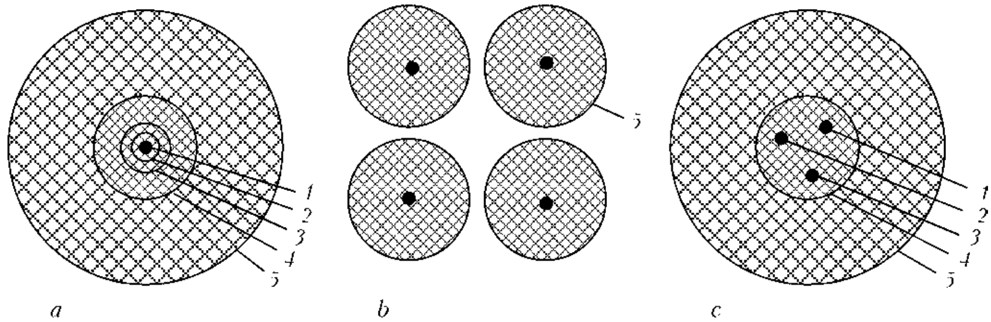

Figure 1. High-voltage cables used in welding guns with cathodes heated by electron bombardment and their parasitic capacitances C_p: *a* — coaxial cable, $C_{p(1-2)}$ = 300, $C_{p(2-3)}$ = 400, $C_{p(3-4)}$ = 500, $C_{p(4-5)}$ = 100 pF/m; *b* — four separate single-core cables, C_p = 70 pF/m; *c* — multi-core cable with conductors in current-conducting screen *4* used as a current conductor to the modulator, $C_{p(1-2)}$ = 150, $C_{p(2-3)}$ = = 70, $C_{p(1,\,2-4)}$ = 210, $C_{p(3-4)}$ = 70, $C_{p(4-5)}$ = 130 pF/m; *1*, *2* — current conductors to heater spiral; *3* — current conductor to cathode; *5* — external grounded screen

ensure a high consistency of the non-through penetration depth in heavy metal sections.

In the majority of cases the high-power (60–120 kW) welding electron guns use massive cathodes heated by electron bombardment, and the most efficient control of the beam current is provided by automatic bias [2], where an electronic valve with grid control is connected to the emission system cathode circuit [3]. In this case, minus of the accelerating voltage source is connected to the modulator (control electrode) of the emission system of the gun.

In the former USSR the guns of this type were equipped with coaxial high-voltage four-core cables of the 4KVEL-60 or 4KVEL-165 grades, and there were no problems with the welding current ripple. But now, because the coaxial cables with the required electric strength between the cores are no longer produced, the use is made of four separate cables (Techmeta, France) or multi-core cables (E.O. Paton Electric Welding Institute). With these cables it is necessary to thoroughly filter the cathode bombardment current to avoid ripple of the welding current, which involves some difficulties associated with placement and reliability of electronic elements at a high potential in oil bath. The bombardment current usually amounts to 100 mA at a voltage of 1.5–5.0 kV. When changing from mains power supply to a supply with a frequency of 20–50 kHz, the effect of ripple of the cathode bombardment current becomes much more pronounced. For example, other conditions being equal, the beam current ripple factor in case of using the bombardment current source with a ripple frequency of 100 Hz is approximately 30 times lower compared to the bombardment current source with a ripple frequency of 20 kHz. The final causes of ripple of the welding electron beam current in the guns considered may be ripples of the accelerating voltage and potential of the modulator (control electrode) of the emission system. As according to the requirements of international standard EN ISO 14744-1 the mean level of the accelerating voltage ripple should not exceed 2 % (in practice it is lower by an order of magnitude), allowing for dependence $I_b \sim U_{acc}^{3/2}$ the value of the beam current ripple for the above reasons should be not higher than 3 %. Apparently, in case of a higher beam current ripple its cause should be looked for in the modulator potential ripple.

Previously, the issues of using different high-voltage cables and associated beam current ripples were not discussed in the technical literature. That gave rise to conducting investigations the results of which are considered below.

Investigation procedure and objects. The high-voltage cables under investigation are shown in Figure 1. When changing from the coaxial cable to other types, we noticed formation of the beam current ripple, which disappeared immediately after a sudden shutdown of the cathode bombardment current (Figure 2). As the cathode cooled down, the beam current gradually fell to zero without any ripple. This result explicitly confirms the fact that the beam current ripple is caused by the cathode bombardment current ripple, but it gives no understanding of the mechanism of this effect and does not allow it to be quantitatively estimated.

Therefore, we used computer mathematical simulation of the beam current control circuits with three types of the high-voltage cables, each 10 m long. Graphic windows of the computer mathematical simulator [4] are shown in Figure 3. They are made so that it is possible to reveal quantitative relationships and main ways of flowing of an alternating component of the cathode bombardment current through parasitic capacitances of a cable. The bombardment voltage source is shown here in the form of two series-connected sources: direct voltage source V2 = 1500 V and alternating voltage source V3 = 1.5–150 V with a frequency ranging from 50 Hz to 50 kHz, which is used to set the ripple factor within the range of interest, i.e. 0.005–0.1. The vacuum diode (heater cathode) is represented by resistor R2 = 20 kOhm = $= U_{bomb}/I_{bomb}$ = 1500 V/0.075 A, which is justified by constancy of the given load. Models of the welding gun and valve GMI-27 were made on the basis of study [5]. Model X5 of welding gun ELA-60-60 corresponds to its modulation characteristic (Figure 4, *a*), and valve model X6 — to the anode characteristic of electronic valve GMI-27 (Figure 4, *b*).

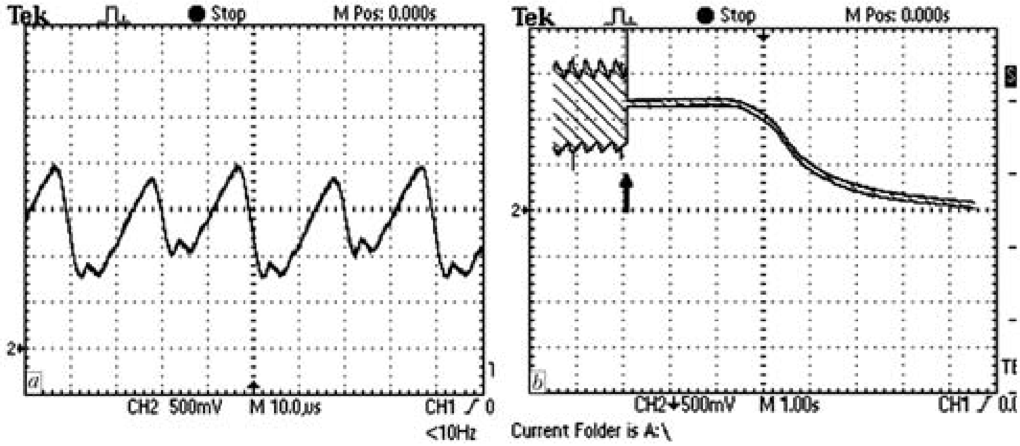

Figure 2. Oscillogram of the beam current ripple (*a*) (time axis scale — one cell = 10 μs) and its termination (*b*) (one cell = 1 s) from the time point of shutoff of the bombardment current when using the multi-core cable. Frequency and ripple factor 50 kHz and 0.28, respectively; time point of shutoff of the bombardment current is marked by an arrow; beam current 12.5 mA; bombardment current 60 mA; bombardment voltage 1.5 kV; oscillograph Tektronix TDS-2002

Results and discussions. In case of using the coaxial cable (see Figure 3, *a*) the alternating component of the bombardment current is closed by the filament-cathode circuit and parasitic capacitance C2, thus exerting no effect on the cathode–modulator potential difference and, hence, beam current ripple. Therefore, in this case there is no need to place the ripple filter at output of the cathode bombardment current source. It is enough just to rectify the bombardment current, as at a frequency of 20–50 kHz the losses in the cable are inadmissibly high. In case of four separate cables (see Figure 3, *b*) the alternating component of the cathode bombardment current is closed both by the filament–cathode circuit and by the accelerating voltage source–ground–parasitic capacitances C1 and C2 circuit shown by the dashed line, where the alternating voltage drop is formed at parallel-connected valve X6 and resistor R5. The latter causes the corresponding beam current ripple. When using the multi-core cable (see Figure 3, *c*), the alternating component of the cathode bombardment current also causes the alternating voltage drop at parallel-connected electronic valve X6 and resistor R5, as there is the circuit of closing of the alternating component of the cathode bombardment current through parasitic capacitances C2–C4.

Figure 5, *a*, *b* shows results of computer simulation of the effect of the beam current on the amplitude of the control voltage and beam current ripples for the same cables at three different bombardment current

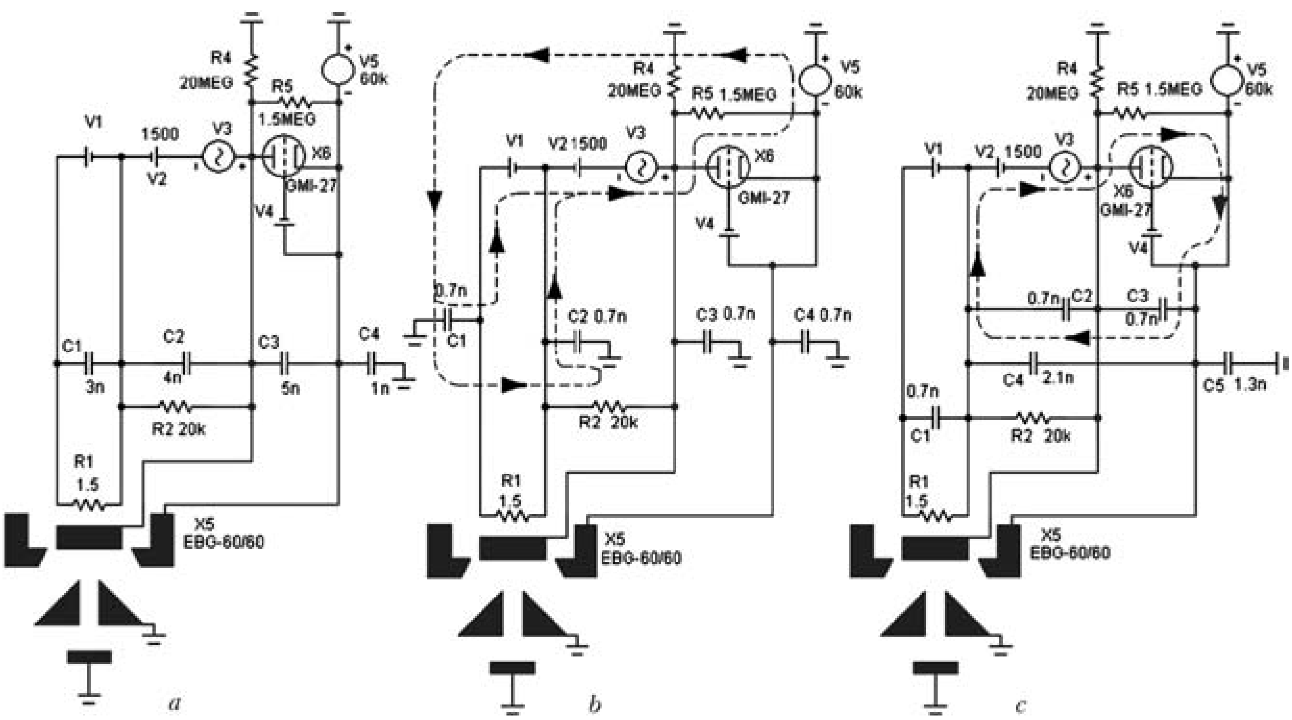

Figure 3. Graphic windows of the computer mathematical simulator of beam current control circuits for coaxial cable (*a*), four separate cables (*b*) and multi-core cable (*c*): VI — heat source for spiral; V2 — source of direct bombardment voltage; V3 — source of alternating voltage; V4 — source of bias voltage; V5 — stabilised source of accelerating voltage; X5 — model of 60 kV and 60 kW welding gun; X6 — simplified model of tetrode GMI-27

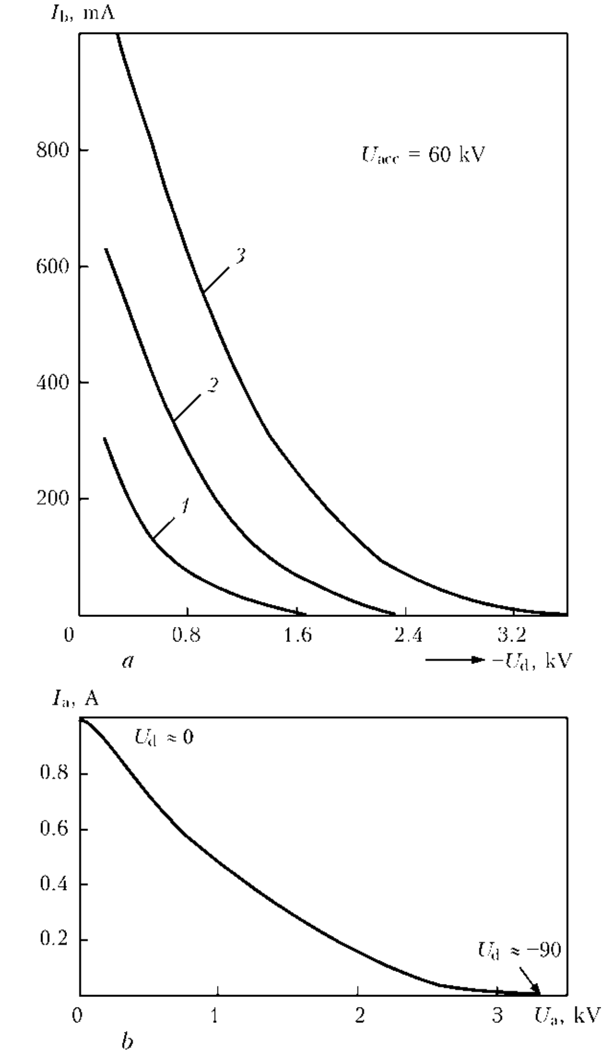

Figure 4. Modulation characteristics of the emission systems forming the beams with currents of 250 (*1*), 500 (*2*) and 1000 (*3*) mA (*a*), and certificate anode characteristic of valve GMI-27 (*b*)

ripple factors. The character of dependencies and, hence, the mechanism of formation of the beam current ripple are identical for both types of the cables, although when using four separate cables the ripple is a bit lower.

As follows from the simulation results, the effect of the bombardment current ripple increases with decrease of the beam current, and at a beam current of 1 mA and cathode bombardment current ripple of 10 % the amplitude of the beam current ripple with a frequency of 20 kHz becomes close to 100 %, which makes functioning of the secondary-electron observation and seam tracking systems impossible. Also, as shown by the above results, to decrease the beam current ripple factor to 0.05 (the maximum permissible value specified by international standard EN ISO 14744-1) it is necessary to limit the cathode bombardment ripple factor formed by the power source at a frequency of 20 kHz to the same value. Connecting an extra capacitance to the circuit between the cathode and modulator provides an efficient decrease of the beam current ripple amplitude, although it deteriorates, accordingly, the dynamic characteristics of the beam current control system.

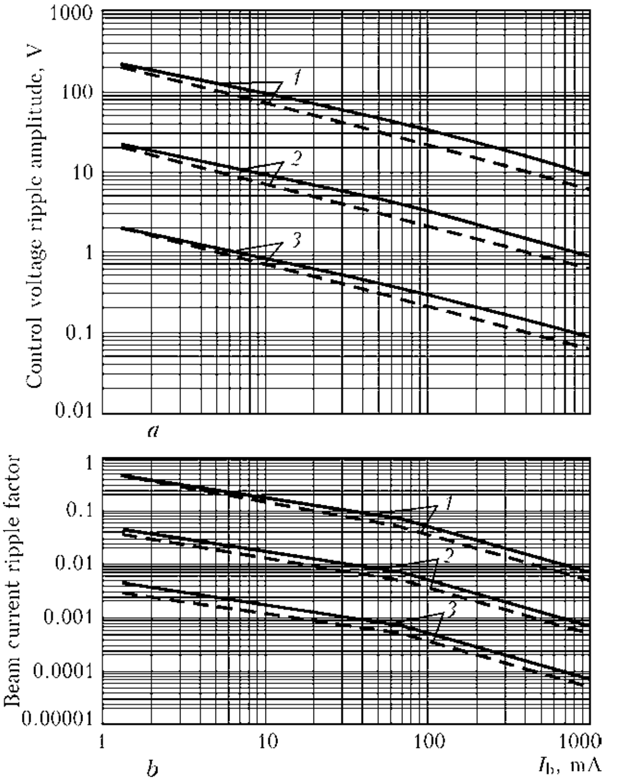

Figure 5. Dependence of the control voltage ripple amplitude (*a*) and beam current ripple factor (*b*) on the beam current when using four separate cables (dashed lines) and multi-core cable (solid lines); bombardment current ripple factor 0.1 (*1*), 0.05 (*2*) and 0.005 (*3*); cathode bombardment current ripple frequency 20 kHz

CONCLUSIONS

1. The cathode bombardment current ripple exerts a substantial effect on the beam current ripple in case of using the multi-core cable or four separate cables, which is caused by parasitic capacitance currents flowing through the beam current control circuit.

2. When using these cables, to decrease the beam current ripple factor to 0.05, which is the maximum permissible value specified by international standard EN ISO 14744-1, it is necessary to limit the cathode bombardment ripple factor at a frequency of 20 kHz to the 0.05 value.

1. *ISO 14744-1*: Welding — acceptance inspection of electron beam welding machines. Pt 1: Principles and acceptance conditions.
2. Rolf, M. *Strahlstromsteuerung fuer eine Elektronenstrahlschweissmachine*. Pat. 24 60 424 Deutsche. Int. Cl. H 01 J 37/24. Publ. March 17, 1977.
3. Nazarenko, O.K., Lanbin, V.S. (2007) Investigation of high-voltage control circuits of welding electron beam current. *The Paton Welding J.*, **5**, 17–20.
4. Amelina, M.A., Amelin, S.A. (2007) *Circuit simulation software Micro-Cap 8*. Moscow: Gor. Liniya Telekom.
5. Koren, N. (1996) Improved vacuum-tube models for SPICE simulation. *Glass Audio*, 8(**5**).